Journal of Biomolecular NMR, 7 (1996) 225–235
ESCOM

J-Bio NMR 347

^{1}H and ^{15}N NMR resonance assignments and solution secondary structure of oxidized *Desulfovibrio desulfuricans* flavodoxin

John R. Pollock[a], Richard P. Swenson[b] and Brian J. Stockman[a,*]

[a]*Pharmacia and Upjohn, Inc., 301 Henrietta Street, Kalamazoo, MI 49001-0199, U.S.A.*
[b]*Department of Biochemistry, The Ohio State University, Columbus, OH 43210, U.S.A.*

Received 2 October 1995
Accepted 24 February 1996

Keywords: Chemical shift index; Flavodoxin; Isotopic enrichment; Nitrogen-15; Protein; Secondary structure; 3D NMR

Summary

Sequence-specific ^{1}H and ^{15}N resonance assignments have been made for 137 of the 146 nonprolyl residues in oxidized *Desulfovibrio desulfuricans* [Essex 6] flavodoxin. Assignments were obtained by a concerted analysis of the heteronuclear three-dimensional ^{1}H-^{15}N NOESY-HMQC and TOCSY-HMQC data sets, recorded on uniformly ^{15}N-enriched protein at 300 K. Numerous side-chain resonances have been partially or fully assigned. Residues with overlapping $^{1}H^{N}$ chemical shifts were resolved by a three-dimensional ^{1}H-^{15}N HMQC-NOESY-HMQC spectrum. Medium- and long-range NOEs, $^{3}J_{NH\alpha}$ coupling constants, and $^{1}H^{N}$ exchange data indicate a secondary structure consisting of five parallel β-strands and four α-helices with a topology similar to that of *Desulfovibrio vulgaris* [Hildenborough] flavodoxin. Prolines at positions 106 and 134, which are not conserved in *D. vulgaris* flavodoxin, contort the two C-terminal α-helices.

Introduction

Flavodoxins are small bacterial electron-transfer proteins that contain a single equivalent of noncovalently bound FMN as their only redox center (Mayhew and Ludwig, 1975). The flavin cofactor has three oxidation states: quinone (oxidized), semiquinone (one-electron reduced), and hydroquinone (two-electron reduced). The redox potentials of both quinone-semiquinone (E_2) and semiquinone-hydroquinone (E_1) for the bound cofactor differ significantly from that of free flavin in solution. Typical E_1 values among flavodoxins from various organisms vary between −320 and −500 mV (Paulsen et al., 1990; Ludwig and Luschinsky, 1992), while that of unbound FMN is −172 mV (Draper and Ingraham, 1968). An understanding of the specific protein–cofactor interactions that alter these redox potentials is paramount to understanding the electron-transfer process.

Structural differences in the flavin binding sites of a variety of flavodoxins have proven difficult to correlate with the dissimilarities in observed redox potentials (Paulsen et al., 1990). This most likely results from the large structural diversity among flavodoxins. However, controlled structural changes induced by a series of single-site mutations in *D. vulgaris* [Hildenborough] flavodoxin have shown that formation of the flavin hydroquinone anion in a hydrophobic environment contributes substantially to the altered E_1 values (Stockman et al., 1994; Swenson and Krey, 1994).

Structural comparison among members of the *Desulfovibrio* family, in the context of redox potentials, provides an excellent complement to the single-site-mutation approach. A number of flavodoxins have been identified from members of this sulfate-reducing genus (Devereux et al., 1990). Amino acid sequences and redox properties are known for *D. desulfuricans* [Essex 6] (Helms and Swenson,

*To whom correspondence should be addressed.

Abbreviations: CSI, chemical shift index; DQF-COSY, double-quantum-filtered correlation spectroscopy; DIPSI, decoupling in the presence of scalar interactions; FMN, flavin mononucleotide; GARP, globally optimized alternating phase rectangular pulse; HMQC, heteronuclear multiple-quantum coherence; HSQC, heteronuclear single-quantum coherence; NOE, nuclear Overhauser effect; NOESY, nuclear Overhauser enhancement spectroscopy; TOCSY, total correlation spectroscopy; TPPI, time-proportional phase increments; TSP, 3-(trimethylsilyl)propionic-2,2,3,3-d_4 acid, sodium salt.

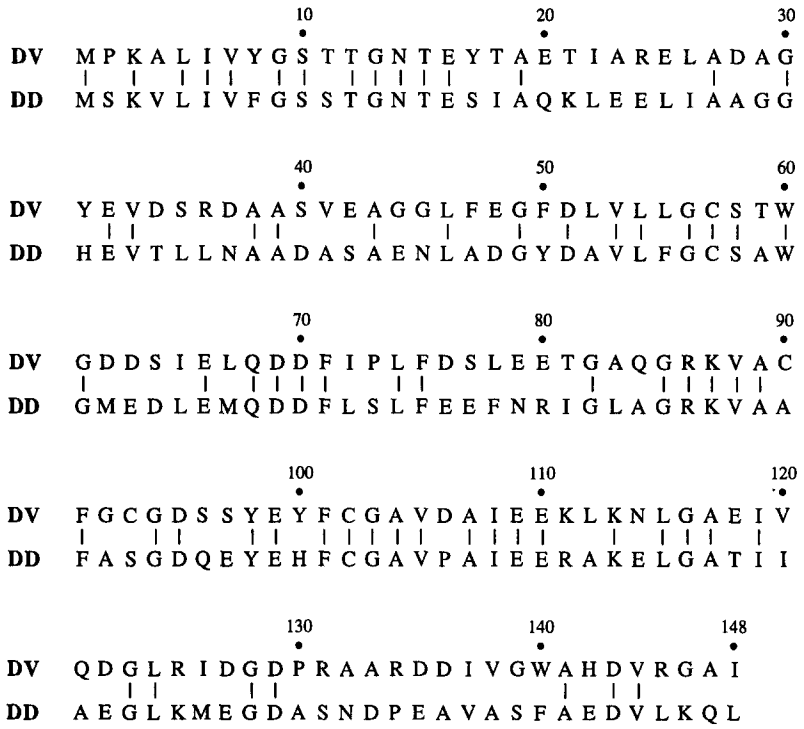

Fig. 1. Amino acid sequence alignment of *D. vulgaris* flavodoxin (DV) and *D. desulfuricans* flavodoxin (DD). Identical residues are marked.

1992), two strains of *D. gigas* (ATCC 29494 and 19364) (Helms and Swenson, 1991), *D. salexigens* (ATCC 14822) (Helms et al., 1990), and *D. vulgaris* (Swenson and Krey, 1994) flavodoxins. A peculiarity of the *Desulfovibrio* family is *D. desulfuricans*. At pH 7.0 its E_2 value is approximately 70 mV more positive than that of *D. salexigens* and about 50 mV more positive than that of *D. gigas*, while its E_1 value is approximately 40 mV more positive than the typical midpoint potential of –440 mV for this family (Helms, 1992). Consequently, *D. desulfuricans* flavodoxin has the widest redox-potential span ($E_2 - E_1$) known for this family of proteins.

As part of our long-term goal to understand the specific protein–cofactor interactions that account for the differences in redox potentials between the various *Desulfovibrio* species, we have used heteronuclear three-dimensional NMR spectroscopy to determine the solution secondary structure of *D. desulfuricans* flavodoxin. The secondary structural results presented here can be compared with those of *D. vulgaris* flavodoxin determined by NMR (Knauf et al., 1993; Stockman et al., 1993) and X-ray crystallography (Watt et al., 1991). Of the *Desulfovibrio* family, *D. desulfuricans* flavodoxin is the least homologous to *D. vulgaris*, having only a 47% residue correspondence, as shown in Fig. 1 (Helms and Swenson, 1991; Swenson and Krey, 1994). Resonance assignments for the wild-type protein also provide a reference point for examining the effects of single amino acid mutations on protein–cofactor interactions in this member of the *Desulfovibrio* family.

Materials and Methods

Protein enrichment and sample preparation

Recombinant *D. desulfuricans* [Essex 6] flavodoxin was expressed in *E. coli* transformed with the Bluescript phagmid containing the 1.8-kb TaqI insert, as previously described (Helms and Swenson, 1991; Helms, 1992). Uniformly ^{15}N-enriched flavodoxin was prepared from M9 minimal medium with $^{15}NH_4Cl$ (Cambridge Isotopes, Andover, MA), supplied as the exclusive source of nitrogen. After elution from the final ion-exchange column, the protein was dialyzed twice against 250 ml of a 10 mM phosphate buffer at pH 6.5. The flavodoxin was lyophilized and dissolved in 40 µl D_2O/400 µl H_2O to a final concentration of 2 mM in a 100 mM phosphate buffer at pH 6.5. A trace amount of NaN_3 was added to prevent bacterial growth. Samples dissolved in D_2O were prepared by lyophilizing the protein and dissolving in 100% D_2O. Some data sets were also recorded on flavodoxin concentrated directly from the ion-exchange eluent (50 mM Tris, 225 mM NaCl, pH 7.3). Under these conditions, several correlations in the ^1H-^{15}N HSQC spectrum exhibited increased intensity.

NMR spectroscopy

All NMR spectra were recorded at 300 K on a Bruker AMX-600 spectrometer equipped with a multichannel interface and operating at a proton frequency of 600.14 MHz. For all experiments recorded in H_2O, continuous-wave low-power saturation was applied during the 1.3-s

relaxation delay to attenuate the H_2O resonance intensity. Proton chemical shifts were referenced to the H_2O signal at 4.76 ppm relative to TSP. Nitrogen chemical shifts were referenced to external 2.9 M $^{15}NH_4Cl$ in 1 M HCl at 24.93 ppm relative to liquid ammonia. Data were processed on a Silicon Graphics Iris 4D/35 or Crimson workstation, using the software package FELIX from Hare Research, Inc. (Woodinville, WA).

Two-dimensional DQF-COSY (Piantini et al., 1982) and NOESY (Kumar et al., 1980) spectra were acquired in H_2O. Proton sweep widths of 9091 Hz were used in each direction. In the 2D DQF-COSY and NOESY experiments, 96 and 160 transients were acquired, respectively, for each of the 256 t_1 increments. Quadrature detection in t_1 was accomplished by TPPI (Marion and Wüthrich, 1983).

The 2D ^1H-^{15}N HSQC spectrum (Bodenhausen and Ruben, 1980) was acquired in H_2O solvent using ^1H and ^{15}N sweep widths of 9091 and 1953 Hz, respectively. For each of 256 t_1 values, 128 transients were recorded. Quadrature detection in t_1 was accomplished by the method of States et al. (1982). GARP decoupling (Shaka et al., 1985) was used to decouple ^{15}N during acquisition. An identical spectrum was recorded within 24 h of exchanging the protein into D_2O.

The 2D ^1H-^{15}N HMQC-J spectrum (Kay and Bax, 1990) was acquired in H_2O solvent using the same sweep widths as described for the previous 2D HSQC spectrum. For each of the 1024 t_1 values, 48 transients were recorded. The acquisition time in t_1 was 262 ms, resulting in a digital resolution of 1.9 Hz/point. During data processing, the t_1 dimension was zero-filled four times for a final spectral resolution of 0.5 Hz/point. Resolution enhancement in t_1 was achieved by using a combination of Gaussian and Lorentzian multiplications. The $^3J_{HN^\alpha}$ values, corrected for the linewidth effect (Kay and Bax, 1990), were extracted by measuring the peak-to-peak separation in the 1D ω_1 projection, corresponding to the center of each correlation in the 2D spectrum.

The 3D ^1H-^{15}N NOESY- and TOCSY-HMQC spectra

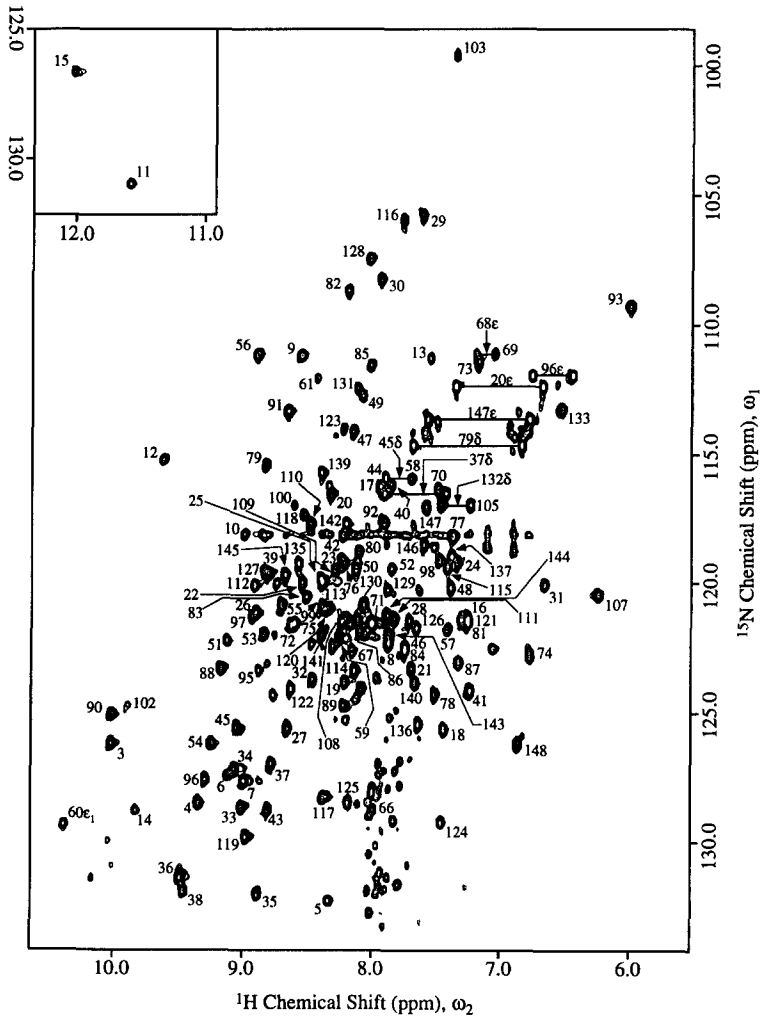

Fig. 2. The 14.2 T ^1H-^{15}N HSQC spectrum of uniformly ^{15}N-enriched *D. desulfuricans* flavodoxin in 100 mM phosphate buffer at pH 6.5. Assigned correlations are labeled according to residue sequence number for main-chain nitrogens or atom type for side-chain nitrogens. Several correlations with narrower line widths and weaker intensity are observed near 8 ppm (^1H) and 130 ppm (^{15}N). Their origin is unclear.

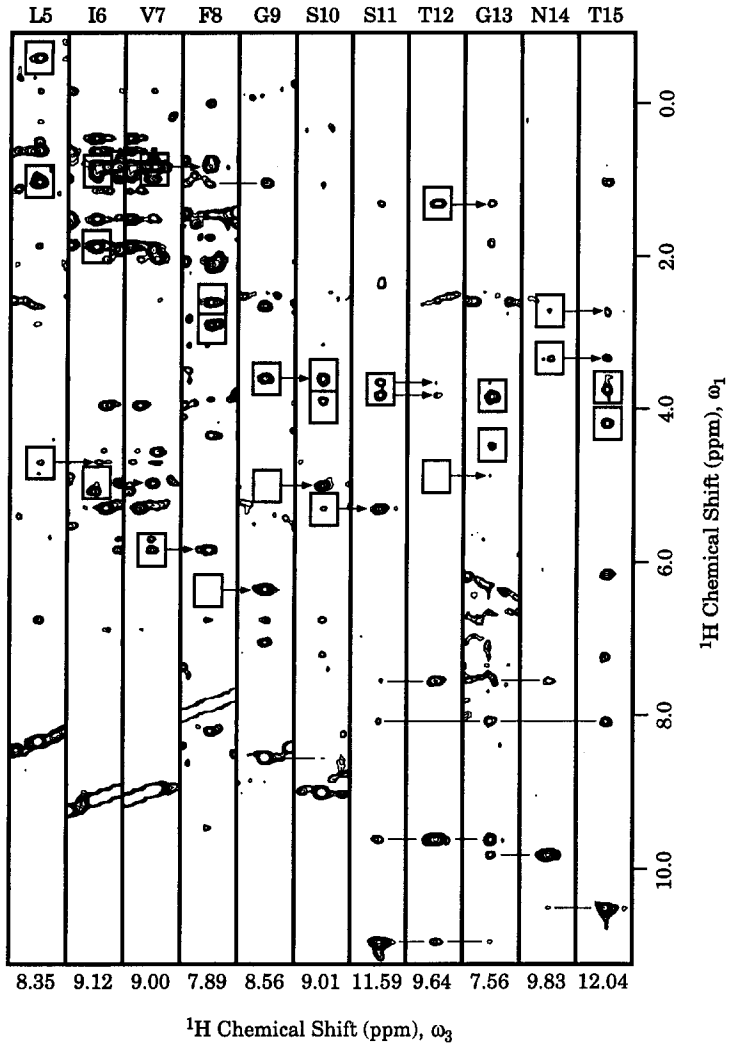

Fig. 3. Selected ω_1,ω_3 slices taken from the 14.2 T 3D ^{1}H-^{15}N NOESY-HMQC spectrum of *D. desulfuricans* in 100 mM phosphate buffer at pH 6.5. Slices are taken at the ^{15}N frequency (see Table 1) corresponding to the residue indicated at the top of each panel. Each slice represents 0.29 ppm in ω_3, with the center located at the indicated $^1H^N$ resonance (see Table 1). Intraresidue $d_{N\alpha}$ and $d_{N\beta}$ correlations are boxed. Sequential $d_{N\alpha}(i,i-1)$ and $d_{N\beta}(i,i-1)$ correlations are indicated by arrows beginning at the preceding intraresidue correlation. Horizontal lines identify d_{NN} or interresidue NOEs. In the Phe[8], Gly[9], Thr[12], and Asn[14] slices the weak intraresidue $d_{N\alpha}$ correlation is not observed. However, a strong correlation is found at the corresponding position in the ^{1}H-^{15}N TOCSY-HMQC spectrum.

were recorded in H_2O solvent (Marion et al., 1989; Zuiderweg and Fesik, 1989). The ω_2 and ω_3 sweep widths were the same as for the ^{1}H-^{15}N HMQC spectrum. The ω_1 sweep width was 7813 Hz, causing foldover of the two downfield-shifted ^{1}H resonances. Reduction of the ω_1 sweep width allowed for enhanced resolution without compounding resonance overlap. Each 3D experiment consists of a series of 2D ^{1}H-^{1}H data sets with incremented ^{15}N evolution periods. Thirty-two scans were recorded for each of 256 t_1 values and 32 t_2 values. Quadrature detection in t_1 and t_2 was accomplished by using TPPI (Marion and Wüthrich, 1983). Decoupling of ^{15}N during t_1 was achieved by a 180° pulse in the center of the evolution period and during acquisition by a GARP sequence (Shaka et al., 1985). A mixing time of 100 ms was used for the NOESY experiment with simultaneous low-power irradiation of the H_2O resonance. A DIPSI-2 (Shaka et al., 1988) spin-lock of 38.5 ms was used for the TOCSY experiment.

The 3D ^{1}H-^{15}N HMQC-NOESY-HMQC spectrum was acquired in H_2O solvent (Frenkiel et al., 1990). Sweep widths were identical to those used for the previous 3D ^{1}H-^{15}N HMQC spectra. Thirty-two transients were recorded for each of 64 t_1 and 64 t_2 values. Quadrature detection in t_1 and t_2 was accomplished by using TPPI (Marion and Wüthrich, 1983). During acquisition, ^{15}N was decoupled with a GARP sequence (Shaka et al., 1985).

Results

The 2D ^{1}H-^{15}N HSQC spectrum of *D. desulfuricans* flavodoxin is shown in Fig. 2. For clarity, the two fur-

thest downfield ^1H correlations, Ser[11] and Thr[15], are displayed in the insert. Two correlations were observed for several residues, most of which are spatially adjacent to the N-terminus of the protein. For some residues the doubling is readily apparent in Fig. 2, while for others, such as Lys[3], the second correlation is too weak to observe at the level shown. Mass spectrometry indicates that this most likely arises from the presence of a mixture of Met[1] and *des*-Met[1] flavodoxin. Conspicuously absent in all ^1H-^{15}N HSQC spectra recorded, regardless of buffer or temperature conditions, was the FMN $^1H^{N3}$ resonance.

Sequential assignment of the backbone resonances of oxidized *D. desulfuricans* flavodoxin was accomplished by the concerted analysis of the 3D ^1H-^{15}N NOESY-HMQC and TOCSY-HMQC data sets. Both data sets were recorded with identical sweep widths, allowing for the corresponding 2D ^1H-^1H slices of each data set to be superimposed, simplifying interpretation. This procedure facilitated differentiation of intraresidue and interresidue correlations for sequential assignment of the residues. In instances of $^1H^N$-$^1H^N$ resonance overlap, $^1H^N$-$^1H^N$ NOEs were assigned by use of the ^1H-^{15}N HMQC-NOESY-HMQC data set.

The 3D data sets were analyzed by a multiple-step process previously described for *D. vulgaris* flavodoxin (Stockman et al., 1993). Alanine and glycine residues, which constitute 25% of the protein, were readily identifiable with only some exceptions. Alanine residues were identified by their intense TOCSY correlations to the $^1H^\beta$ methyl group, whereas glycine residues were identified by their characteristic ^{15}N chemical shift and two TOCSY correlations to the $^1H^\alpha$ resonances. Periodically, aromatic amino acid side chains could be distinguished by virtue of a $^1H^N$-$^1H^\delta$ NOE in the region around 7.0 ppm. Magnetization transfer in the TOCSY-HMQC data set allowed for the identification of the $^1H^\beta$ proton(s) in most cases and occasionally extended further down the side chain.

An example of the sequential assignment process is shown for residues 5–15 in Fig. 3. By sequence homology to *D. vulgaris* flavodoxin, these residues form numerous hydrogen bonds to the flavin phosphate group, securing FMN to the protein (Watt et al., 1991; Stockman et al., 1993). The $^1H^N$ chemical shifts of these residues for *D. vulgaris* and *D. desulfuricans* flavodoxins are similar, typified by the downfield shifts of Ser[11] and Thr[15]. Low-field chemical shifts for these amide protons have been encountered in other flavodoxins (Clubb et al., 1991; Stockman et al., 1993) and are attributed to strong hydrogen bonding to the oxygen atoms of the FMN phosphate group. Sequential $d_{N\alpha}(i,i-1)$ correlations were seen for all residues, except for Asn[14] and Thr[15]. Sequential d_{NN} correlations were observed for these two residues, as well as for the preceding three residues.

In several instances, pairs of residues contained degenerate or nearly degenerate $^1H^N$ chemical shifts, prohibiting

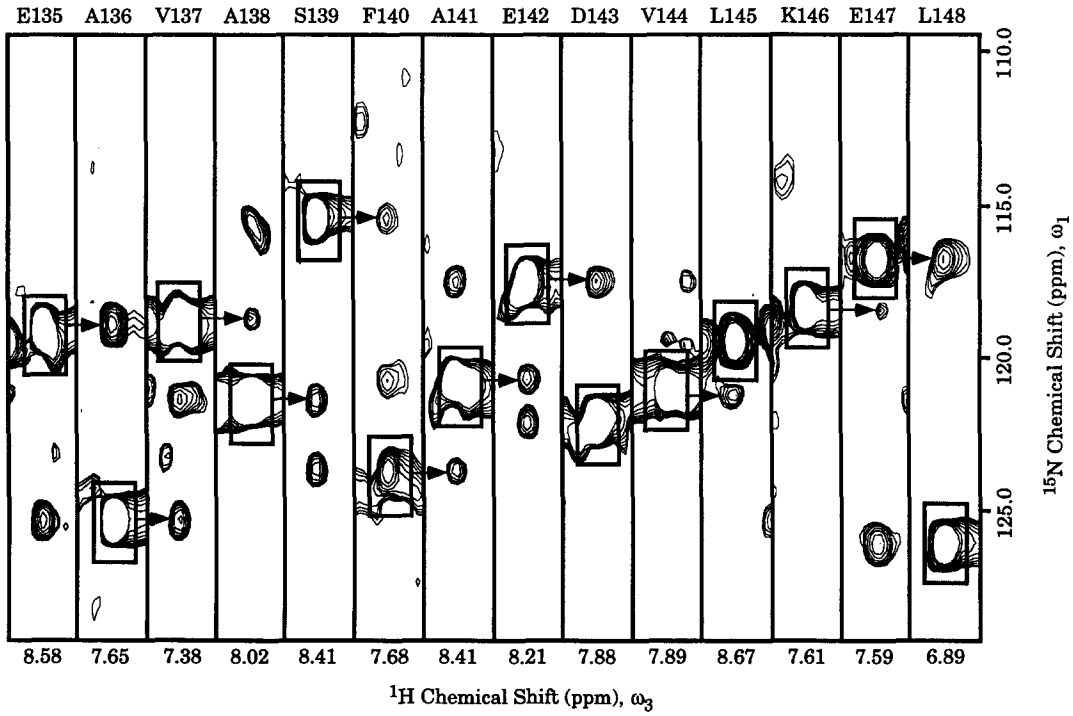

Fig. 4. Selected ω_1,ω_3 slices taken from the 14.2 T 3D ^1H-^{15}N HMQC-NOESY-HMQC spectrum of *D. desulfuricans* in 100 mM phosphate buffer at pH 6.5. Slices are taken at the ^{15}N frequency (see Table 1) corresponding to the residue indicated at the top of each panel. Each slice represents 0.44 ppm in ω_3, with the center located at the indicated $^1H^N$ resonance (see Table 1). The one-bond ^1H-^{15}N correlation for each residue is boxed. Sequential d_{NN} correlations are indicated by arrows beginning at the boxed ^1H-^{15}N correlation in the preceding slice.

TABLE 1
ASSIGNED ^{1}H AND ^{15}N CHEMICAL SHIFTS FOR *D. desulfuricans* FLAVODOXIN[a]

Residue	N^{α}	H^{N}	H^{α}	H^{β}	Others	Residue	N^{α}	H^{N}	H^{α}	H^{β}	Others
Met[1]						Gly[56]	111.2	8.90	1.51, 4.31		
Ser[2]			4.28	3.73, 3.89		Cys[57]	121.8	7.41	3.92	1.18, 1.91	
Lys[3]	126.2	10.02	5.40	1.51, 1.84		Ser[58]	116.0	7.69	3.38	2.19	
	126.1[b]	9.84[b]	5.29[b]			Ala[59]	122.2	8.28	3.81	0.96	
Val[4]	128.5	9.34	4.83	1.87	H^{γ} 0.61	Trp[60]					$H^{\delta 1}$ 6.31; $H^{\varepsilon 1}$ 10.40;
	128.4[b]	9.40[b]									$N^{\varepsilon 1}$ 130.7
Leu[5]	132.3	8.35	4.71	1.03	H^{γ} −0.59	Gly[61]	112.1	8.44	3.95		
	132.3[b]	8.38[b]				Met[62]					
Ile[6]	127.4	9.12	4.98	1.87	$H^{\gamma 1}$ 0.79; $H^{\gamma 2}$ 0.99	Glu[63]					
Val[7]	127.6	9.00	5.84	1.87	H^{γ} 0.72	Asp[64]					
Phe[8]	122.3	7.89	6.36	2.61, 2.90		Leu[65]					
Gly[9]	111.2	8.56	3.60, 5.01			Glu[66]	128.8	8.01	4.61	1.50, 2.19	
Ser[10]	118.1	9.01	5.32	3.68, 3.90		Met[67]					
Ser[11]	131.0	11.59	3.82	3.66		Gln[68]					H^{ε} 7.06, 7.21; N^{ε} 111.2
Thr[12]	115.2	9.64	4.89		H^{γ} 1.32	Asp[69]	111.2	7.05			
Gly[13]	111.3	7.56	3.84, 4.51			Asp[70]	116.5	7.50	4.39	2.24, 3.17	
Asn[14]	128.8	9.83	4.53	2.76, 3.33		Phe[71]	121.6	8.00	3.64	2.85, 3.50	H^{δ} 7.05
Thr[15]	126.7	12.04	3.77	4.17		Leu[72]	121.6	8.64	3.93	1.83	
Glu[16]	121.2	7.25	4.43	2.70		Ser[73]	111.4	4.10	3.82		
Ser[17]	116.3	7.95	4.25	3.73		Leu[74]	122.8	6.78	4.05	1.32	
Ile[18]	125.6	7.46	3.40	1.87	H^{γ} 0.51	Phe[75]	121.6	8.63	3.77	2.93	H^{δ} 6.23; H^{ε} 7.05
Ala[19]	123.8	8.23	3.46	1.24		Glu[76]	119.2	8.23	3.88	2.05	
Gln[20]	116.6	8.34	3.89	2.10	H^{γ} 2.29; H^{ε} 6.69,7.35;	Glu[77]	118.2	7.41	3.91	1.68, 2.28	
					N^{ε} 112.4	Phe[78]	124.3	7.53	4.14	2.52, 3.02	H^{δ} 6.85
Lys[21]	123.3	7.70	4.21	1.73, 1.88		Asn[79]	115.4	8.84	4.20	2.53, 2.79	H^{δ} 6.85, 7.69;
Leu[22]	120.0	8.57	3.77	1.78							N^{δ} 114.7
Glu[23]	119.1	8.27	3.61			Arg[80]	118.8	8.11	4.44	1.74, 2.01	H^{γ} 1.68; H^{δ} 3.12;
Glu[24]	119.2	7.40	3.91	2.24							H^{ε} 7.70; N^{ε} 84.7
Leu[25]	119.7	8.41	4.02	1.65		Ile[81]	121.7	7.26	4.43	1.72	
Ile[26]	121.2	8.88	3.89	1.78	H^{γ} 0.58	Gly[82]	108.7	8.21	3.89, 4.33		
Ala[27]	125.6	8.66	4.59	1.52		Leu[83]	120.5	8.52	3.74	1.36, 1.60	
Ala[28]	121.5	7.72	4.21	1.51		Ala[84]	122.7	7.75	3.82	1.42	
Gly[29]	105.8	7.64	3.54, 4.35			Gly[85]	111.5	8.02	3.84, 4.15		
Gly[30]	108.2	7.94	3.64, 3.97			Arg[86]	121.5	8.12	4.63	1.58, 1.70	H^{γ} 1.58; H^{δ} 2.93, 3.28;
His[31]	120.0	6.67	4.86	2.35, 3.00							H^{ε} 6.91; N^{ε} 86.5
	119.7[b]	6.58[b]				Lys[87]	123.1	7.35	4.84	1.96	H^{γ} 1.23
Glu[32]	123.7	8.47	4.56	2.06, 2.28		Val[88]	123.3	9.18	5.69	1.73	H^{γ} 0.99
Val[33]	128.7	8.98	5.29	2.03	H^{γ} 0.84	Ala[89]	124.7	8.23	5.05	1.54	
Thr[34]	127.2	9.07	4.56	3.96	H^{γ} 1.14	Ala[90]	125.1	10.02	6.25	1.45	
Leu[35]	132.1	8.87	5.09	1.92	H^{γ} 1.21	Phe[91]	133.5	8.66	5.47	2.42, 2.65	H^{δ} 6.70
Leu[36]	131.4	9.50	4.63	1.60		Ala[92]	117.6	7.92	3.87	1.10	
Asn[37]	126.9	8.79	3.15	2.44, 2.80	H^{δ} 7.43, 7.90;	Ser[93]	109.3	6.01	4.99	3.56	
					N^{δ} 116.5	Gly[94]					
Ala[38]	131.9	9.47	3.58	1.05		Asp[95]	123.0	8.81	5.37	3.05	
Ala[39]	119.6	8.79	4.00	1.13		Gln[96]	127.6	9.30	3.61	1.59	H^{δ} 1.14, 1.61; H^{ε} 6.45,
Asp[40]	116.2	7.84	3.74	2.56, 2.88							6.76; N^{ε} 112.0
Ala[41]	123.6	7.24	4.40	1.18		Glu[97]	121.3	8.92	3.82	1.49, 1.90	
Ser[42]	118.1	8.26	4.58	3.76		Tyr[98]	119.1	7.49	3.98	2.33, 2.88	H^{δ} 6.72
Ala[43]	128.8	8.79	3.63	1.36		Glu[99]	120.9	8.41	3.88	1.58, 1.86	
Ala[47]	114.1	8.17	4.23	1.09		His[100]	117.0	8.64	3.66	3.03	
Asp[48]	120.2	7.40	4.21	2.61		Phe[101]	129.6	8.48		2.87, 3.35	H^{δ} 7.20
Gly[49]	112.8	8.10	3.53, 3.90			Cys[102]	124.7	9.89	3.79	2.02	
Tyr[50]	119.5	8.14	4.40	2.65, 2.89	H^{δ} 6.75	Gly[103]	99.6	7.29	3.39, 3.60		
	119.7[b]	8.15[b]				Ala[104]	125.5	8.54	3.58	1.35	
Asp[51]	122.2	9.13	5.67	2.56, 2.88		Val[105]	117.0	7.18	4.28	1.69	
	122.1[b]	9.24[b]				Pro[106]					
Ala[52]	119.5	7.86	5.60	0.98		Ala[107]	120.5	6.26	4.11	1.10	
Val[53]	122.0	8.85	4.86	1.45	H^{γ} −0.15, 0.51	Ile[108]	121.5	8.24	3.51	1.86	
Leu[54]	126.2	9.25	5.54	1.46, 1.86		Glu[109]	119.5	8.29	3.72	2.29	
Phe[55]	120.8	8.70	5.72	2.99, 3.23	H^{δ} 7.31	Glu[110]	117.7	8.47	4.00	1.74	

TABLE 1
(continued)

Residue	N^{α}	H^N	H^{α}	H^{β}	Others	Residue	N^{α}	H^N	H^{α}	H^{β}	Others
Arg^{111}	121.4	7.84	4.22	2.00	H^{γ} 1.26, 1.47; H^{δ} 2.85, 3.31; H^{ε} 7.09; N^{ε} 86.3	Asn^{132}	122.6	8.15	4.10	2.93, 3.14	H^{γ} 7.24, 7.47; N^{γ} 117.0
						Asp^{133}	113.3	6.55	4.91	2.47, 3.28	
Ala^{112}	120.1	8.91	4.02	1.47		Pro^{134}					
Lys^{113}	120.1	8.39	4.23	1.96		Glu^{135}	119.2	8.58	4.10	2.09	H^{γ} 2.33
Glu^{114}	123.4	8.15	4.10	2.40		Ala^{136}	125.5	7.65	4.14	1.47	
Leu^{115}	119.4	7.42	4.38	1.78		Val^{137}	119.0	7.38	3.46	2.07	H^{γ} 0.74
Gly^{116}	105.9	7.77	3.87, 4.33			Ala^{138}	121.6	8.02	3.95	1.45	
Ala^{117}	128.3	8.38	4.86	1.24		Ser^{139}	115.7	8.41	4.20	4.02	
Thr^{118}	117.3	8.55	4.42	3.83	H^{γ} 1.11	Phe^{140}	123.9	7.68	4.58	3.03, 3.31	H^{γ} 7.26
Ile^{119}	129.8	8.99	5.08	2.15	H^{γ} 1.04	Ala^{141}	122.0	8.41	3.41	1.32	
Ile^{120}	121.0	8.37	4.28			Glu^{142}	117.7	8.21	3.87	2.14	
Ala^{121}	121.5	7.27	4.43	1.08		Asp^{143}	122.0	7.88	4.35	2.61, 2.90	
Glu^{122}	124.1	8.64	4.23	2.03, 2.37		Val^{144}	121.3	7.89	3.07	1.77	H^{γ} 0.43
Gly^{123}	114.1	8.24	3.36, 4.56			Leu^{145}	119.7	8.67	3.62	2.01	
Leu^{124}	129.3	7.47	4.16	0.28, 0.88		Lys^{146}	118.5	7.61	4.12	1.96	
Lys^{125}	128.5	8.21	4.61	1.75	H^{γ} 0.81, 1.12		118.6[b]	7.53[b]			
Met^{126}	121.8	7.67	5.00			Gln^{147}	117.0	7.59	4.53	1.70, 2.43	H^{γ} 1.96, 2.39; H^{ε} 6.85, 7.69; N^{ε} 114.7
Glu^{127}	119.5	8.84	5.27	1.97, 2.16							
Gly^{128}	107.5	8.02	3.64, 4.00				117.0[b]	7.64[b]			
Asp^{129}	120.3	7.90	4.58	3.07		Leu^{148}	126.2	6.89	4.02	0.90, 1.31	
Ala^{130}	116.4	8.05	3.84	1.19			125.9[b]	6.84[b]			
Ser^{131}	112.5	8.13	4.16	3.93		FMN					H^{N3} 10.57; N^3 160.5

[a] Proton chemical shifts are ±0.02 ppm. Nitrogen chemical shifts are ±0.1 ppm.
[b] A second set of resonances was identified for this residue.

identification of potential $^1H^N$-$^1H^N$ NOE connectivities. Although not necessarily essential for assignment purposes, these NOEs are beneficial for confirming sequence assignments and providing additional secondary structure information. The 3D ^1H-^{15}N HMQC-NOESY-HMQC (Frenkiel et al., 1990) spectrum, with ^{15}N in both the ω_1 and ω_2 dimensions, was acquired to identify these NOEs. The $^1H^N$-$^1H^N$ NOEs are found in the ω_3 dimension at the $^1H^N$ chemical shift of one residue and in the ω_1 dimension at the ^{15}N chemical shift of the second residue. The NOE is easily identified, provided that the ^{15}N frequencies are not degenerate. Figure 4 illustrates the correlations identified in this data set for residues 135–148. The observation of strong $^1H^N$-$^1H^N$ NOEs throughout this sequence indicates that this stretch of residues adopts an α-helical conformation.

In total, 137 of the 146 nonproline amino acids have been assigned. A list of all assigned resonances is presented in Table 1. A summary of the observed sequential and medium-range NOEs, $^1H^N$ solvent exchange properties and $^3J_{NH^{\alpha}}$ coupling constants is shown in Fig. 5.

Discussion

The solution secondary structure of *D. desulfuricans* flavodoxin was determined from analysis of a 3D ^1H-^{15}N NOESY-HMQC data set by identifying medium-range NOEs, indicative of helical and turn conformations, and long-range NOEs that define β-strands. Resonance degeneracy and/or weak intensities prohibited assignment of several $d_{N\alpha}(i,i-3)$ NOEs, such as in the two middle α-helices. Additional information about the secondary structure was obtained from $^1H^N$ solvent exchange properties and $^3J_{NH^{\alpha}}$ coupling constants. Collectively, the criteria delineate a five-stranded β-sheet framework and four α-helices.

Strong d_{NN} NOEs, weak $d_{N\alpha}(i,i-3)$ NOEs, $^3J_{NH^{\alpha}}$ values less than 6 Hz, and reduced $^1H^N$ exchange rates identified four α-helices, comprising residues 16–28, 69–81, 104–117, and 131–148. The α-helix spanning residues 69–81 is less characteristic, exhibiting strong d_{NN} NOEs but only a few $d_{N\alpha}(i,i-3)$ correlations. Lack of observation of $d_{N\alpha}(i,i-3)$ correlations does not arise because of $^1H^{\alpha}$ resonance degeneracy (Table 1). The pattern of reduced $^1H^N$ exchange rates is sporadic for this α-helix. This is identical to what was observed for the corresponding α-helix in *D. vulgaris* flavodoxin (Stockman et al., 1993), and indicates that this α-helix is flexible in solution. It is interesting to note that the $^3J_{NH^{\alpha}}$ values for Glu^{77} and Arg^{80} in both *D. vulgaris* and *D. desulfuricans* flavodoxin are greater than 8 Hz, further supporting the notion that in both proteins this helix is quite flexible. The α-helix spanning residues 104–117 is also less characteristic, exhibiting strong d_{NN} NOEs but only a few $d_{N\alpha}(i,i-3)$ correlations. In this case, however, lack of observation of $d_{N\alpha}(i,i-3)$ correlations does result from $^1H^{\alpha}$ resonance degeneracy (Table 1). In contrast to the 69–81 α-helix, here the pattern of reduced $^1H^N$ exchange rates is very pronounced. Pro^{106}, however, dis-

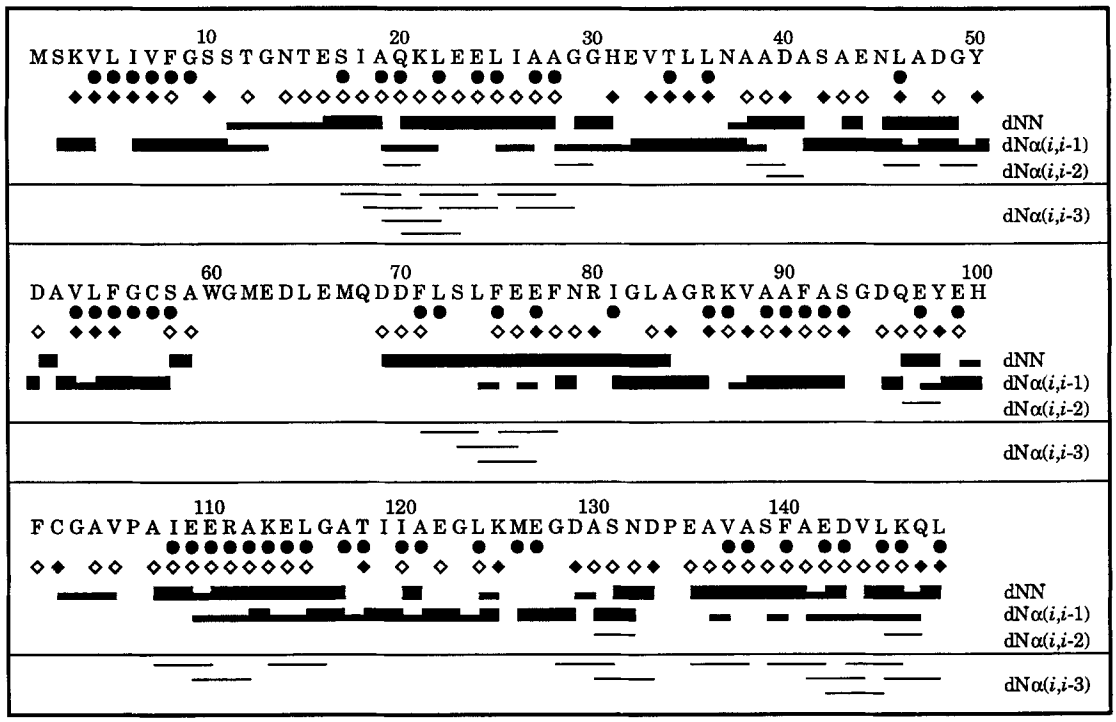

Fig. 5. Summary of sequential resonance assignments of *D. desulfuricans* flavodoxin. A filled circle indicates that the $^1H^N$ proton was still detectable after 24 h in D_2O. Diamonds below residues signify $^3J_{HN^\alpha}$ values of less than 6 Hz (open) or greater than 8 Hz (filled). A bar between two residues indicates that a d_{NN} or $d_{N\alpha}(i,i-1)$ NOE was observed between the two residues. Strong-intensity NOEs are signified by wide bars, whereas weak- or medium-intensity NOEs are signified by narrow bars. Observed medium-range $d_{N\alpha}(i,i-2)$ and $d_{N\alpha}(i,i-3)$ NOEs are indicated with horizontal lines between the involved residues.

rupts the N-terminal portion of this α-helix, resulting in the absence of slowly exchanging $^1H^N$ resonances at this end of the α-helix compared to the corresponding α-helix in *D. vulgaris* flavodoxin (Stockman et al., 1993). The remaining two α-helices have NMR characteristics (Fig. 5) very similar to their counterparts in *D. vulgaris* flavodoxin, despite the low sequence homology in these regions of the two flavodoxins (Stockman et al., 1993).

The α-helices from both *D. vulgaris* and *D. desulfuricans* flavodoxin align remarkably well (Watt et al., 1991; Knauf et al., 1993; Stockman et al., 1993), their origins and terminations differing by only 1–2 residues, as defined by d_{NN} NOEs and $^3J_{NH^\alpha}$ values. The only major differences between the α-helices in *D. vulgaris* and *D. desulfuricans* flavodoxin are caused by the presence of Pro^{106} and Pro^{134} in the latter protein. These two proline residues are not conserved in *D. vulgaris* flavodoxin. Both of these residues occur near the beginning of their corresponding α-helices and distort the N-terminal ends. As shown in Fig. 5, residues at the beginnings of these two α-helices are still characterized by d_{NN} NOEs, weak $d_{N\alpha}(i,i-3)$ NOEs or $^3J_{NH^\alpha}$ values less than 6 Hz, despite the presence of the proline residue.

Twenty-three long-range $^1H^N$-$^1H^N$ or $^1H^N$-$^1H^\alpha$ NOEs between backbone resonances, indicative of β-sheet structure, were identified. Residues involved in β-sheet structure were also characterized by reduced $^1H^N$ solvent exchange rates, $^3J_{NH^\alpha}$ values greater than 8 Hz, strong $d_{N\alpha}(i,i-1)$ correlations, and low-field $^1H^N$, $^1H^\alpha$, and $^{15}N^\alpha$ chemical shifts. Analysis of the interstrand NOEs resulted in alignment of five parallel β-sheet strands with a β-sheet connectivity of β_2-β_1-β_3-β_4-β_5, as illustrated in Fig. 6. Comparison of the *D. desulfuricans* flavodoxin β-sheet structure with that of *D. vulgaris* flavodoxin shows an identical arrangement of five parallel β-strands. In addition, nearly identical regions of the linear amino acid sequence comprise the β-sheet framework of each protein (Watt et al., 1991; Knauf et al., 1993; Stockman et al., 1993).

Identification of $d_{N\alpha}(i,i-2)$ NOEs for residues Gly^{30}, Asp^{40}, Ala^{41}, Ala^{47}, Tyr^{50}, Tyr^{98} and Asn^{132} (Fig. 5) indicates that conformational tight turns are located at these positions (Richardson, 1981; Wagner et al., 1986; Wüthrich, 1986; Wagner, 1990). Observed d_{NN} NOEs indicate that residues 27–30 and 37–41 are type I turns.

Comparison of the secondary structure for *D. vulgaris* and *D. desulfuricans* as defined by the chemical shift index (Wishart et al., 1992) is illustrated in Fig. 7. Coils and open arrows represent α-helix and β-sheet, respectively. Comparison of the CSI plots indicates that only minor differences in secondary structure exist between the two flavodoxins. In fact, the correspondence of the CSI between the two flavodoxins is quite remarkable. While the two proteins are 47% identical in the linear amino acid

sequence, they are 74% identical in their CSI values (98 out of 132 residues for which the $^1H^{\alpha}$ resonances are assigned in both proteins). The effect of secondary structure on chemical shift is conserved, with different amino acid types at structurally homologous positions experiencing similar secondary-structure-dependent chemical shifts.

The secondary structure of *D. desulfuricans* flavodoxin, determined here by multinuclear NMR spectroscopy, is in good agreement with a model proposed by Caldeira et al. (1994). The *D. desulfuricans* flavodoxin amino acid sequence reported by Caldeira et al. (1994) is different, but highly homologous (79% identical), to that of the *D. desulfuricans* flavodoxin used in the present study, indicating that the two *D. desulfuricans* flavodoxins are from slightly different strains. Their model was derived using the X-ray crystallographic structure of *D. vulgaris* flavodoxin as a starting point. The linear amino acid sequence of *D. vulgaris* was replaced with that of *D. desulfuricans* flavodoxin and the resulting structure was subjected to energy minimization. The NMR data presented here suggests that similar models can be built for other members of the *Desulfovibrio* family, which typically have about 50% sequence homology, with good reliability. Given the high sequence homology, each member of the *Desulfovibrio* family likely adopts the same global fold in solution.

The flavin cofactor $^1H^{N3}$ resonance was not observed in any of the 2D ^1H-^{15}N HSQC spectra recorded. A weak $^1H^{N3}$ resonance was observed in the 3D ^1H-^{15}N NOESY-HMQC spectra, but did not give rise to any NOE connectivities. Presaturation of the H_2O resonance may be partially responsible, but this has not been a problem with other flavodoxins we have studied (Stockman et al., 1994). Another possible explanation is the ability of the protein–cofactor complex to spontaneously self-reduce during data acquisition, forming a mixture of oxidation states. The mechanism by which this occurs is unclear at this time. However, this phenomenon may be related to the more positive reduction potentials of this flavodoxin and the unusually slow reoxidation rates by molecular oxygen in air-saturated buffers (L.R. Helms and R.P. Swenson, 1992; unpublished observations). This idea is supported by the absence of a resonance for Gly^{94}, which is hydrogen-bonded to FMN in the semiquinone state for *D. vulgaris* (Watt et al., 1991), as well as weaker intensities observed for residues 13–15, 58–61 and 100–103 adjacent to the cofactor binding site. Redox-state and/or conformational heterogeneity may thus be hampering our ability to observe resonances from the flavin cofactor and nearby residues. Future experiments may be conducted under an atmosphere of 100% oxygen or in the presence of inorganic oxidizers in order to maintain fully oxidized protein.

Interestingly, the consensus flavin-binding site residues, comprising two loops of the protein that interact with the flavin isoalloxazine ring, residues 56–68 and 92–103, are not identically conserved between the *D. vulgaris* and *D. desulfuricans* flavodoxins (Fig. 1). Some significant differences exist, including methionine residues at positions 62

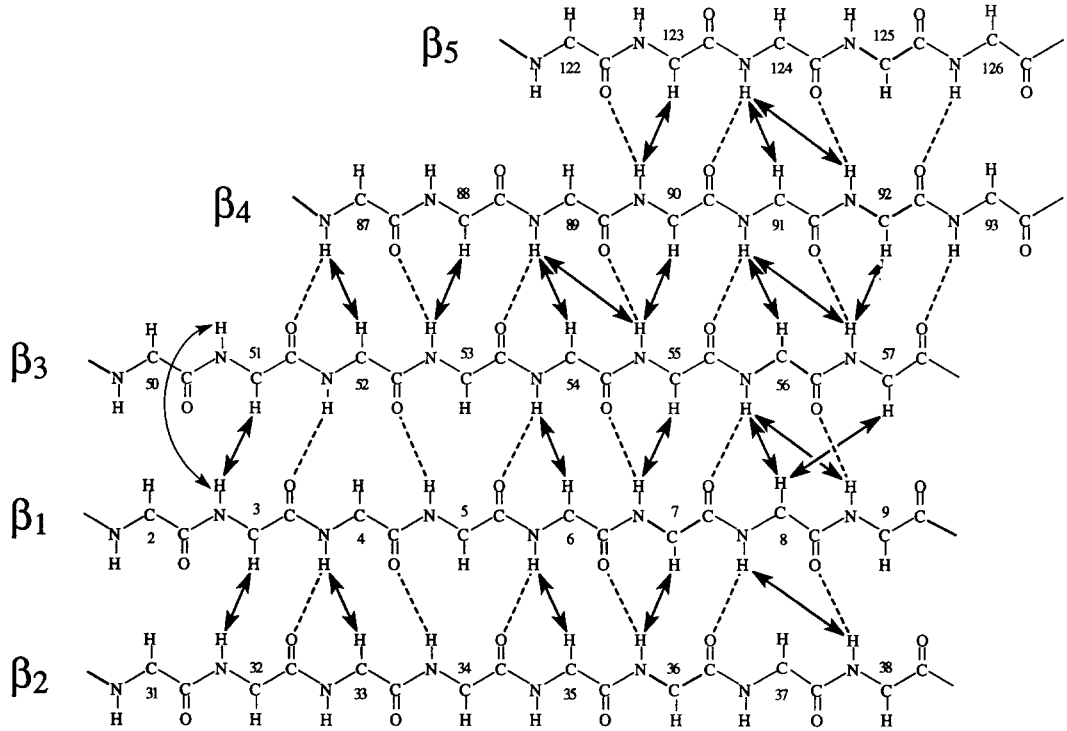

Fig. 6. Schematic diagram of the five-stranded parallel β-sheet arrangement of *D. desulfuricans* flavodoxin. Double-headed arrows identify interstrand NOEs. Dashed lines indicate interstrand hydrogen bonding inferred from analysis of $^1H^N$ exchange in D_2O.

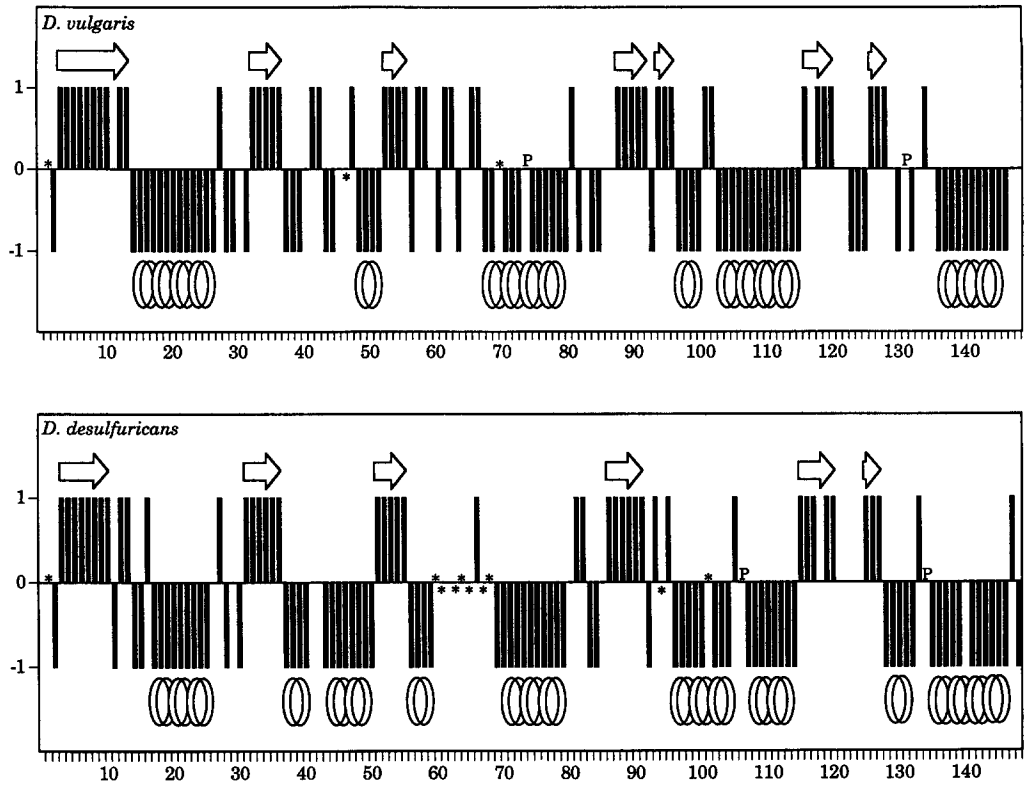

Fig. 7. Comparison of the chemical shift index of $^1H^\alpha$ protons for the *D. vulgaris* and *D. desulfuricans* flavodoxins. Predicted α-helices and β-strands are shown by coils and open arrows, respectively. An asterisk indicates residues for which no $^1H^\alpha$ resonance was assigned. Proline residues in each flavodoxin are denoted with a 'P'.

and 67 in *D. desulfuricans* flavodoxin that correspond to aspartic acid and leucine residues, respectively, at these positions in *D. vulgaris* flavodoxin; aspartic acid and glutamic acid residues instead of serine residues at positions 64 and 97, respectively; and a histidine residue rather than a tyrosine residue at position 100. These differences could be partially responsible for the pronounced differences in the midpoint potentials of *D. desulfuricans* flavodoxin relative to those of the other members of the *Desulfovibrio* family. The electrostatic environment surrounding the FMN cofactor has been directly demonstrated by site-directed mutagenesis to markedly affect the redox potentials of the cofactor (Swenson and Krey, 1994; Zhou and Swenson, 1995). Also, preliminary results suggest that replacing the tyrosine with a histidine residue at position 100 causes the midpoint potential for the E_1 couple to increase significantly (Helms, 1992; unpublished results). Structural differences certainly account for the differences in redox potentials between these two flavodoxins and most likely are responsible for the differences in reoxidation in the presence of oxygen. Work in progress may lead to a structural understanding of these phenomena.

Acknowledgements

This work was supported in part by NIH Grant GM-36490 (R.P.S.). We thank Dr. Lubomyr Baczynskyj for providing the mass spectrometry data and Michael Fairbanks for HPLC support.

References

Bodenhausen, G. and Ruben, D.L. (1980) *Chem. Phys. Lett.*, **69**, 185–188.

Caldeira, J., Palma, P.N., Regalla, M., Lampreia, J., Calvete, J., Schäfer, W., LeGall, J., Moura, I. and Moura, J.J.G. (1994) *Eur. J. Biochem.*, **220**, 987–995.

Clubb, R.T., Thanabal, V., Osborne, C. and Wagner, G. (1991) *Biochemistry*, **30**, 7718–7730.

Devereux, R., He, S.-H., Doyle, C.L., Orkland, S., Stahl, D.A., LeGall, J. and Whitman, W.B. (1990) *J. Bacteriol.*, **172**, 3609–3619.

Draper, R.D. and Ingraham, L.L. (1968) *Arch. Biochem. Biophys.*, **125**, 802–808.

Frenkiel, T., Bauer, C., Carr, M.D., Birdsall, B. and Feeney, J. (1990) *J. Magn. Reson.*, **90**, 420–425.

Helms, L.R., Krey, G.D. and Swenson, R.P. (1990) *Biochem. Biophys. Res. Commun.*, **168**, 809–817.

Helms, L.R. and Swenson, R.P. (1991) *Biochim. Biophys. Acta*, **1089**, 417–419.

Helms, L.R. (1992) Ph.D. Thesis, The Ohio State University, Columbus, OH.

Helms, L.R. and Swenson, R.P. (1992) *Biochim. Biophys. Acta*, **1131**, 325–328.

Kay, L.E. and Bax, A. (1990) *J. Magn. Reson.*, **86**, 110–126.

Knauf, M.A., Löhr, F., Curley, G.P., O'Farrell, P., Mayhew, S.G., Müller, F. and Rüterjans, H. (1993) *Eur. J. Biochem.*, **213**, 167–184.

Kumar, A., Ernst, R.R. and Wüthrich, K. (1980) *Biochem. Biophys. Res. Commun.*, **95**, 1–6.

Ludwig, M.L. and Luschinsky, C.L. (1992) In *Chemistry and Biochemistry of Flavoenzymes*, Vol. 3 (Ed., Müller, F.), CRC Press, Boca Raton, FL, pp. 427–466.

Marion, D. and Wüthrich, K. (1983) *Biochem. Biophys. Res. Commun.*, **113**, 967–974.

Marion, D., Driscoll, P.C., Kay, L.E., Wingfield, P.T., Bax, A., Gronenborn, A.M. and Clore, G.M. (1989) *Biochemistry*, **28**, 6150–6156.

Mayhew, S.G. and Ludwig, M.L. (1975) In *The Enzymes*, Vol. 12 (Ed., Boyer, P.), Academic Press, New York, NY, pp. 57–117.

Paulsen, K.E., Stankovich, M.T., Stockman, B.J. and Markley, J.L. (1990) *Arch. Biochem. Biophys.*, **280**, 68–73.

Piantini, U., Sørensen, O.W. and Ernst, R.R. (1982) *J. Am. Chem. Soc.*, **104**, 6800–6801.

Richardson, J.S. (1981) *Adv. Protein Chem.*, **34**, 167–339.

Shaka, A.J., Barker, P.B. and Freeman, R. (1985) *J. Magn. Reson.*, **64**, 547–552.

Shaka, A.J., Lee, C.J. and Pines, A. (1988) *J. Magn. Reson.*, **77**, 274–293.

States, D.J., Haberkorn, R.A. and Ruben, D.J. (1982) *J. Magn. Reson.*, **48**, 286–292.

Stockman, B.J., Euvrard, A., Kloosterman, D.A., Scahill, T.A. and Swenson, R.P. (1993) *J. Biomol. NMR*, **3**, 133–149.

Stockman, B.J., Richardson, T.E. and Swenson, R.P. (1994) *Biochemistry*, **33**, 15298–15308.

Swenson, R.P. and Krey, G.D. (1994) *Biochemistry*, **33**, 8505–8514.

Wagner, G., Neuhaus, D., Wörgötter, E., Vasák, M., Kägi, J.H.R. and Wüthrich, K. (1986) *J. Mol. Biol.*, **187**, 131–135.

Wagner, G. (1990) *Prog. NMR Spectrosc.*, **22**, 101–139.

Watt, W., Tulinsky, A., Swenson, R.P. and Watenpaugh, K.D. (1991) *J. Mol. Biol.*, **218**, 195–208.

Wishart, D.S., Sykes, B.D. and Richards, F.M. (1992) *Biochemistry*, **31**, 1647–1651.

Wüthrich, K. (1986) *NMR of Proteins and Nucleic Acids*, Wiley, New York, NY.

Zhou, Z. and Swenson, R.P. (1995) *Biochemistry*, **34**, 3183–3192.

Zuiderweg, E.R.P. and Fesik, S.W. (1989) *Biochemistry*, **28**, 2387–2391.